

## 5.1 ELECTRON-MOLECULAR ION INTERACTION

M. Larsson, Å. Larson, A. Le Padellec, S. Rosèn, J. Semaniak, C. Strömholm,  
*Physics Dept., KTH, S-100 44 Stockholm, Sweden*

S. Datz,  
*ORNL, Oak Ridge, TN, USA*

W. Van der Zande, R. Peverall  
*FOM, Amsterdam, The Netherlands*

J. Peterson  
*MPL, SRI International, Menlo Park, USA*

H. Danared, G. H. Dunn, M. Af Ugglas  
*Manne Siegbahn Laboratory*

### 1 Introduction

The long storage times in heavy ion rings make them excellent tools to study intramolecular processes. Depletion of excited vibrational levels by radiative decay and well defined collision energy are the main advantages in studies of molecular ion - electron collisions [1,2,3]. In the last year the experiments concerned the following aspects of electron - molecular ion interactions: absolute cross sections for dissociative recombination (DR) as well as dissociative excitation (DE) and kinetic energy release in DR process. The study of product state distribution in DR of diatomic molecular ions has been successfully initialized by means of a method of translational spectroscopy.

### 2 Dissociative recombination

#### 2.1 Cross sections

The molecular group has recently performed a DR study of the  $D_3^+$  ion, which is a heavy isotopomer of  $H_3^+$  with the same electronic structure. The  $H_3^+$  ion has been recently detected in two interstellar clouds [4] and is believed to play the central role in the chemistry of these natural plasmas. The  $H_3^+$  saga has been previously described elsewhere [5], so that a brief overview will be given here. For the so-called DR direct process to occur efficiently, a favorable curve crossing is needed between the ionic and the dissociative potential curves; this is not the case for the DR of a cold  $H_3^+$  ion. To account for the manifold experimental evidences of its DR high efficiency at low energy, a new theory has emerged

over the last couple of years, although no detailed calculations have been carried out. The new mechanism is called the tunneling mode and is based on non-adiabatic couplings between the inner wall of the dissociative state ( $X^2E'$ ) of  $H_3$  and the ionic potential curve.

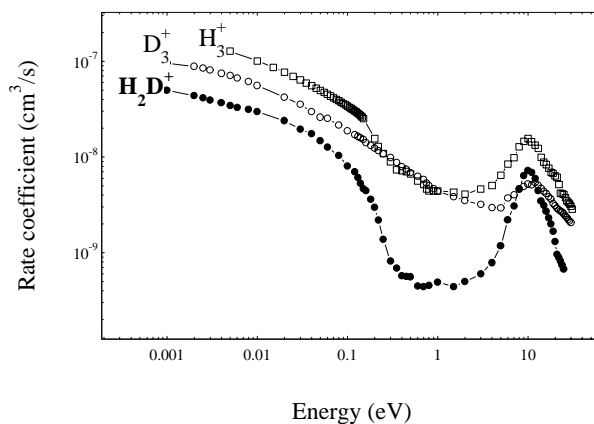


Figure 1. The absolute dissociative recombination rate coefficients measured for  $H_3^+$ ,  $H_2D^+$  and  $D_3^+$ .

Nevertheless, it is expected that the tunneling mode should be less efficient for  $D_3^+$  than for  $H_3^+$ , because doubling the mass of the ion should reduce dramatically the rate of quantum tunneling through the barrier. One of our purposes was to check this prediction and the efficiency of the  $D_3^+$  dissociative recombination has effectively been measured to be a factor of four smaller than the one of  $H_3^+$ . Another point was the search for a field effect which was previously found to influence some Canadian measurements [6] on  $H_3^+$ ; some highly excited Rydberg

states involved in the recombination process were field ionized during their passage through an electrostatic deflector. We did not observe any evidence of field effect in our  $D_3^+$  study.

Very recently, we have also looked into an ion of particular atmospheric interest:  $N_2^+$ . For instance, its dissociative recombination is believed to be responsible for the escape of atomic nitrogen fragments from the Martian atmosphere, when their kinetic energy is sufficient. Due to their lack of any dipole moment (infrared inactive molecules), vibrationally excited ions produced in a conventional source do not relax in the storage ring prior to the recombination measurements. Nevertheless and thanks to the new operating JIMIS hollow cathode source, we were able to produce relatively cold  $N_2^+$  ions. This has been confirmed by the dissociative excitation data (threshold location) as well as by the 3D imaging data (see below). Our results are in perfect agreement with most of the other experimental results, which indicate a fairly high efficiency for the dissociative recombination of slightly excited  $N_2^+$  ions. An accepted value of the corresponding rate coefficient at room temperature would be  $2 \cdot 10^{-7} \text{ cm}^3 \text{ s}^{-1}$ . Contrary to the  $H_3^+$  case, the direct DR process is quite efficient for  $N_2^+$  due to the presence of different dissociative routes in the vicinity of the  $v=0$  level.

## 2.2 Imaging spectroscopy

The kinetic energy release in the dissociative recombination process was measured for  $^3\text{HeD}^+$  for incident energies between 0 and 15 eV [7]. It was found that the  $\text{He}(1s^2)+D(n=2)$  channel completely dominates at zero electron energy. The data are in agreement with MQDT calculation that predict the dissociation route via  $C^2\Sigma^+$  state, leading to the situation that the asymptotic state  $D(n=2)$  totally dominates. At collision energies above 10 eV, many channels leading to excited He atoms were found to contribute and a strong angular anisotropy of the dissociation products is observed.

The imaging spectroscopy has been used to measure the kinetic energy release in dissociative recombination of  $\text{OH}^+$ . It has been found that the metastable  $a^1\Delta$  state is populated in the beam even after the storage time of 10 s. Unfortunately, calculations give a lifetime of 0.1s which disagrees completely with our statement. Our measurements permitted to calculate a new experimental value of the

$a^1\Delta$  state excitation energy of 2.25 eV which is in good agreement with an electron spectroscopy measurement by Katsumata and Lloyd [8].

A three-dimensional, position-sensitive imaging detector has been used to measure the atomic limits and vibrational features of the DR process with  $N_2^+$ . A vibrational distribution of ions produced in the hollow cathode source JIMIS has been found to be  $v=0$  (55%),  $v=1$  (23%),  $v=2$  (13%) and  $v=3$  (10%).

## 3 Dissociative excitation

In the dissociative excitation process an electron excites an ion to a repulsive ionic state and thus results in dissociation. An alternative pathway is when a doubly excited neutral state is formed which then autoionizes to the vibrational continuum of the ground state ion. Both mechanisms of DE have been studied in CRYRING for  $^4\text{HeH}^+$  [9] and  $D_3^+$  molecular ions. Absolute cross sections measured for

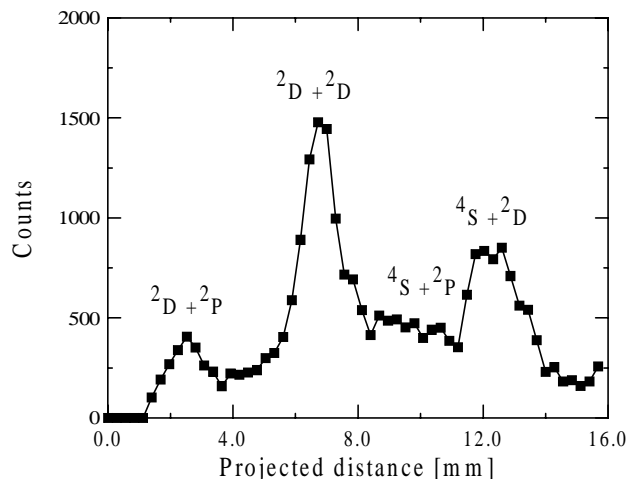


Figure 2. The distribution of projected distances between two nitrogen atoms following DR of  $N_2^+$ .

the ( $^4\text{He}^++\text{H}$ ) and ( $^4\text{He}+\text{H}^+$ ) dissociation channels show step rises at energies corresponding to vertical excitation energies from the ground state to the excited ionic states (19 and 30 eV, respectively). The peak found in the ( $^4\text{He}+\text{H}^+$ ) channel is due to an electron capture to Rydberg series converging to the first excited  $a^3\Sigma^+$  and  $A^1\Sigma^+$  ionic states, that then autoionize. This finding has been confirmed by the theoretical calculations by Orel and Kulander. In the case of  $D_3^+$  both dissociation channels (containing  $D_2$  and  $D$ , respectively) seem to have the same threshold for the direct excitation at about 14 eV. The low energy peak found in the  $D_2$  channel at an

energy of 8 eV arises probably as a result of a competition between dissociation and autoionization of the resonant neutral states formed in the electron capture process.

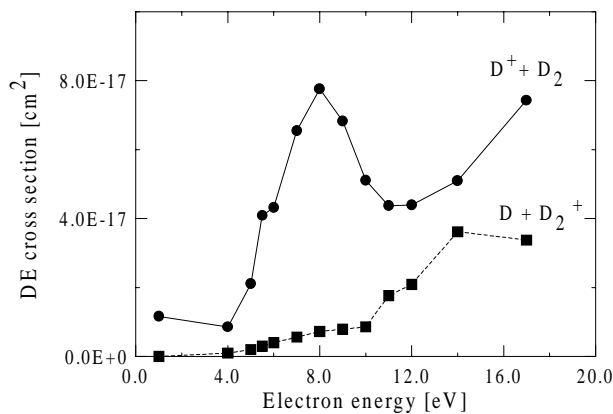


Figure 3. The absolute dissociative excitation cross sections measured for  $D_3^+$ .

#### 4 Development of an imaging detector

An imaging detector for molecular fragmentation has been developed [10]. It is a time and position sensitive detector that determines both the transversal separation and the difference in time of arrival of molecular fragments. The detector has been used first time in December 96 to study dissociative recombination of  $N_2^+$ . Then the kinetic energy release in the reaction and hence the quantum states of the fragments have been measured.

The main part of the detector is a stack of three micro channel plates (MCP) and a phosphorous screen. The neutral particles, created in a DR event, produce a bunch of electrons in the MCP that are further accelerated to the phosphorous screen. The fluorescence light from the screen is detected by a charge couple device (CCD) camera. The frames are analyzed to find the position and the transversal

separation of fragments according to the beam axis. To measure the difference in time of arrival there are a number of gold strips evaporated on the rear side of the last MCP. By fast electronics it is possible to measure the time difference from pulse from separate strips (fast preamplifier and constant fraction discriminator (CFD) and analog to digital converter (ADC)).

The spatial resolution of the camera is 160  $\mu\text{m}$  as best and the time resolution is about 300 ps.

#### 5 References

- [1] M. Larsson, "Dissociative recombination in ion storage rings", *Int. J. Mass Spectrom. Ion Proc.* **149/150** (1995) 403.
- [2] M. Larsson, "Atomic and molecular physics with ion storage rings", *Rep. Prog. Phys.* **58** (1995) 1267.
- [3] M. Larsson, "Atomic physics with ion storage rings", *Physics World* **40** (1996) 916.
- [4] T. R. Geballe and T. Oka, *Nature* **384**, (1996) 334.
- [5] N. G. Adams and D. Smith, "Rate Coefficients in Astrochemistry", Kluwer, Dordrecht, (1988) 173.
- [6] J. B. A. Mitchell, M. Bogelstad and F.B. Yousif, unpublished
- [7] C. Strömholm, J. Semaniak, S. Rosèn, H. Danared, S. Datz, W. Van der Zande, and M. Larsson, "Dissociative recombination and dissociative excitation of  $^4\text{HeH}^+$ : Absolute cross-sections and mechanisms", *Phys. Rev. A* **54** (1996) 3086.
- [8] Katsumata S. and Lloyd D.R., *Chem. Phys. Let.* **45**, 519 (1977)
- [9] J. Semaniak, S. Rosèn, G. Sundström, S. Datz, H. Danared, M. af Ugglas, M. Larsson, and W. Van der Zande, Z. Amitay, D. Zajfman, U. Hechtfisher, M. Grieser, R. Repnow, M. Schmidt, D. Schwalm, and A. Wolf, "Product state distributions in dissociative recombination of  $^3\text{HeD}^+$ ", *Phys. Rev. A* **54** (1996) R4617
- [10] S. Rosèn, "Software and hardware of the CRYRING three dimensional detector", KTH 1996